Journal of Nuclear Materials 389 (2009) 497–499

Contents lists available at ScienceDirect

Journal of Nuclear Materials

journal homepage: www.elsevier.com/locate/jnucmat

Letter to the Editor

Radiation damage effects in the uranium-bearing δ-phase oxide $Y_6U_1O_{12}$

M. Tang [a,*], K.S. Holliday [b], J.A. Valdez [a], B.P. Uberuaga [a], P.O. Dickerson [a], R.M. Dickerson [a], Y. Wang [a], K.R. Czerwinski [b], K.E. Sickafus [a]

[a] *Materials Science and Technology Division, Los Alamos National Laboratory, Mail-Stop G755, P.O. Box 1663, Los Alamos, NM 87545, USA*
[b] *Radiochemistry Group, University of Nevada, Las Vegas, NV 89154, USA*

ARTICLE INFO

Article history:
Received 8 December 2008
Accepted 2 February 2009

PACS:
81.05.Je
61.80.Jh
61.16.Bg
61.05.Cp
61.50.Ks

ABSTRACT

Ion irradiation damage effects in delta (δ) $Y_6U_1O_{12}$ were characterized using grazing incidence X-ray diffraction and transmission electron microscopy. Experimental results revealed no amorphization transformation occurs in Kr-ion irradiated $Y_6U_1O_{12}$ to a maximum displacement damage dose of ~50 displacements per atom at cryogenic temperature. Density functional theory calculations indicate that δ-$Y_6U_1O_{12}$ possesses a relatively low cation antisite formation energy, which may help to explain the observed resistance of δ-$Y_6U_1O_{12}$ to irradiation-induced amorphization of δ-$Y_6U_1O_{12}$.

To develop advanced nuclear fuel forms or waste forms, the search for radiation-tolerant materials has been an area of intense research in recent years [1–4]. The purpose of this study is to examine the radiation damage behavior of complex actinide oxides whose structures are similar to fluorite. The particular actinide compound of interest in this report is delta (δ) phase $Y_6U_1O_{12}$. The crystal structure of δ-$Y_6U_1O_{12}$ is closely related to the cubic fluorite structure [5,6], but possesses rhombohedral (not cubic) symmetry and belongs to space group $R\bar{3}$. Many M_7O_{12} compounds (including $A_6B_1O_{12}$ and $A_4B_3O_{12}$ stoichiometries) are known to crystallize in the rhomobohedral δ-phase structure [7]. The δ-$Y_6U_1O_{12}$ structure is interesting because it is completely analogous to another fluorite derivative structure know as pyrochlore, a structure typical of compounds with $A_2B_2O_7$ stoichiometry, for which numerous radiation damage studies have been reported (see, e.g., Refs. [2–4]). Both $A_2B_2O_7$ pyrochlores and $A_6B_1O_{12}$ δ-phase compounds are characterized by ordered A/B arrangements on the cation sublattice along with ordered arrangements of vacancies on the anion sublattice (see Sickafus et al., for a comprehensive comparison of the pyrochlore and δ-phase structures [8]). We report here that δ-$Y_6U_1O_{12}$ exposed to heavy ion irradiation at cryogenic temperature does not amorphize, but undergoes a partial order-to-disorder (O–D) transformation at a relatively high displacement damage dose.

Y_2O_3 powder (99.9%) from Alpha Aesar calcined at 1000 °C for 12 h, was mixed with UO_2 powder from Bio-Analytical Industries, in the molar ratio of 1:3, then ball milled in a stainless steel cup and pressed to a pressure of 6 tons in a SPEX 13 mm die. These pressed pellets were then oxidized in air in a Mellen high temperature tube furnace, initially for 4 h at 350 °C, then at 1500 °C for 12 h. X-ray diffraction (XRD) measurements indicated that unreacted Y_2O_3 and UO_2 remained in these pellets after these sintering steps. Consequently, pellet fragments from these samples were subsequently annealed in a box furnace for 72 h at 1000 °C under air, then re-milled, repressed and re-sintered in air at 1500 °C for 72 h. XRD measurements on these samples showed that the sintered pellets consisted primarily of δ-$Y_6U_1O_{12}$. Ion irradiations were performed at cryogenic temperature (~100 K) in the Ion-Beam Materials Laboratory at Los Alamos National Laboratory, using a Varian ion implanter operating at 150 kV. About 300 keV Kr^{++} ions were implanted at normal incidence using a dose rate of 1×10^{16} Kr/m^2 s to fluences ranging from 0.5 to 2×10^{20} Kr/m^2. Irradiated samples were analyzed using both grazing incidence X-ray diffraction (GIXRD) and transmission electron microscopy (TEM). GIXRD measurements were performed using a Bruker AXS D8 Advanced X-ray diffractometer at a gracing incidence angle of $\alpha = 0.25°$. Irradiated samples were prepared in cross-sectional geometry for TEM examination using a focused-ion-beam (FIB) apparatus. TEM investigations were performed using a Philips CM-30 instrument operating at 300 kV.

Fig. 1 shows GIXRD patterns obtained from pristine δ-$Y_6U_1O_{12}$ and $Y_6U_1O_{12}$ irradiated with 300 keV Kr^{++} ions to fluences of 5×10^{19} Kr/m^2 and 2×10^{20} Kr/m^2. These ion fluences correspond to peak displacement damage doses of ~12 and 50 dpa (these are estimates based on the Monte Carlo ion transport code SRIM [9]; 40 eV was used for the displacement threshold energy for all target atoms in these calculations). The pristine GIXRD pattern in Fig. 1 is

---

[*] Corresponding author. Tel.: +1 505 665 1472; fax: +1 505 667 8021.
E-mail address: mtang@lanl.gov (M. Tang).

0022-3115/$ - see front matter © 2009 Elsevier B.V. All rights reserved.
doi:10.1016/j.jnucmat.2009.02.001

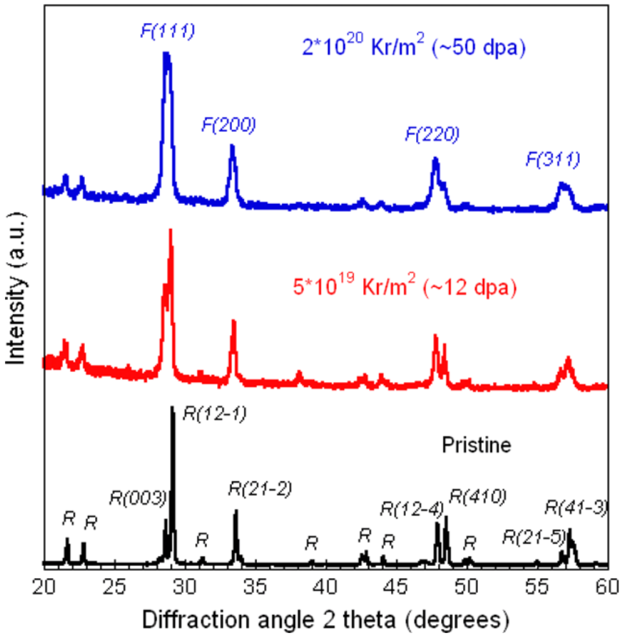

Fig. 1. Grazing incidence X-ray diffraction (GIXRD) patterns obtained from $Y_6U_1O_{12}$ before and after irradiation with 300 keV Kr^{++} ions at 100 K. The angle of incidence of the X-rays for these measurements was $\alpha = 0.25°$.

consistent with the rhombohedral δ-phase $Y_6U_1O_{12}$ structure (diffraction peaks labeled '*R*'). As for the GIXRD patterns obtained from the Kr^{++} ion irradiated samples, one important observation is that there are no apparent broad diffraction features, attributable to an amorphous structure, even at the highest experimental dose. This observation suggests that no ion-irradiated induced amorphization occurs in $Y_6U_1O_{12}$, at least to ~50 dpa. Interestingly, with increasing ion irradiation fluence the diffraction peaks are observed to broaden and the weakest δ-phase peaks decrease in intensity more than the four most prominent diffraction peaks (at ~29°, 34°, 48°, 57° 2θ). These four major diffraction maxima peaks are associated with the 'parent' fluorite structure (diffraction peaks labeled '*F*'), while the weaker peaks are due to the special structural arrangement associated with the fluorite derivative, δ-phase structure. The diminishing intensities of the weaker δ-phase reflections with increasing ion irradiation dose, suggest that the $Y_6U_1O_{12}$ is gradually undergoing an order-to-disorder (O–D) transformation from an ordered δ-phase $Y_6U_1O_{12}$ structure to a disordered fluorite structure. The broadening of the diffraction maxima with increasing irradiation dose is due either to decreased grain size or increased lattice strain.

It is difficult to quantify the extent of the O–D transformation of $Y_6U_1O_{12}$, based on the GIXRD measurements described above. The problem is that the 300 keV Kr^{++} ions have a relatively limited range in $Y_6U_1O_{12}$ (~200 nm, based on SRIM calculations) and we are not certain that the low angle of X-ray grazing incidence used in these GIXRD measurements, $\alpha = 0.25°$, is sufficiently low to ensure that we are sampling only the irradiated surface layer. We estimate that $\alpha = 0.25°$ is less than the critical angle, α_c, for $Y_6U_1O_{12}$, based on the critical angle formula from Guinier [10] ($\alpha_c = 0.35°$). This suggests that our GIXRD measurements are only probing a very thin layer of near surface materials (~ few nanometers), much less than the range of the Kr^{++} ions. However, a geometric alternative method for calculating X-ray penetration as a function of X-ray incidence angle [11], suggests that we are sampling to a depth of ~50 nm in $Y_6U_1O_{12}$ for incidence angle $\alpha = 0.25°$. In summary, we cannot say for sure whether or not our GIXRD measurements avoid sampling the unirradiated bulk material.

Fig. 2 shows a cross-sectional TEM image obtained from $Y_6U_1O_{12}$ irradiated with 300 keV Kr^{++} ions to a fluence of 2×10^{20} Kr/m^2 (corresponding to ~50 dpa). The microdiffraction (μD) patterns indicate no diffuse halo (which would be expected from an amorphous structure), but a change in structure is apparent between the unirradiated substrate (bottom μD pattern) and the irradiated layer (top μD patterns). The substrate μD pattern is consistent with the rhombohedral δ-phase $Y_6U_1O_{12}$ structure with $\vec{B} = [2\,1\,1]$ (using the three-index system for indexing hexagonal directions). Superlattice reflections associated with the rhombohedral δ-phase are seen to partially or completely disappear in the top μD patterns obtained from different irradiated areas. Those brighter, fundamental reflections in the μD patterns from the irradiated layer can be indexed as consistent with a cubic, disordered fluorite phase oriented with $\vec{B} = [\bar{1}\,1\,2]$. These TEM observations indicate that the O–D transformation of $Y_6U_1O_{12}$ is only partially complete by the highest Kr^{++} ion dose of ~50 dpa.

To summarize the experimental results, GIXRD and TEM observations indicate a partial irradiation-induced phase transformation in $Y_6U_1O_{12}$ from an ordered, δ-phase structure with rhombohedral symmetry to a disordered fluorite phase with cubic symmetry by the highest experimental dose of ~50 dpa. We interpret this transformation to the cubic fluorite phase as an O–D transformation, analogous to that seen in previous radiation damage studies on the 6:1:12 δ-phase compounds $Y_6W_1O_{12}$ and $Yb_6W_1O_{12}$ [12,13] and other 4:3:12 δ-phase compounds [4,14]. For irradiated δ-phase compounds, cation antisite defects form on the cation sublattice and anion Frenkel defects are created on the anion sublattice. As these defect concentration grow, the rhombohedral symmetry of the ordered δ-phase vanishes in favor of cubic symmetry. Eventually, the material transforms to a structure indistinguishable from the fluorite (CaF_2) crystal structure. We refer to this radiation-induced structure as a 'disordered fluorite' phase. Pyrochlore ($A_2B_2O_7$) compounds undergo an O–D transformation from an ordered fluorite derivative structure to a disordered fluorite phase under irradiation (see, e.g. [3]). The O–D transformation observed in $A_2B_2O_7$ pyrochlores is analogous to the O–D transformation observed in $A_6B_1O_{12}$ δ-phase compounds, in that in both cases, the transformation occurs as a result of cation antisite and anion Frenkel defect formation and accumulation.

It is interesting that our δ-$Y_6U_1O_{12}$ ion irradiation results suggest substantial amorphization resistance, since this compound remains crystalline to a dose of 50 dpa, while isostructural compounds δ-$Y_6W_1O_{12}$ [12] and δ-$Yb_6W_1O_{12}$ [13] are amorphized under the same irradiation conditions. In previous studies, we have proposed that point defect formation energies have significant effects on the susceptibility of complex oxides to radiation damage, in particular, to radiation-induced amorphization [2,4]. Under irradiation, the lattice energy increases rapidly, especially in materials with high defect formation energies. When the free energy of the defective crystalline structure during irradiation exceeds the free energy of the aperiodic state, the material should succumb to an amorphization transformation.

To gain some insight into the defect processes responsible for disordering and amorphization under irradiation, we performed density functional theory (DFT) calculations to estimate the energy required to create an antisite pair in $Y_6U_1O_{12}$ and uranium surrogate δ-phase compounds, $Y_6W_1O_{12}$ and $Yb_6W_1O_{12}$. The DFT calculations were performed with the Vienna Ab Initio Simulation Package (VASP) [15] using the projector augmented wave (PAW) method [16]. Exchange and correlation effects were treated within the generalized gradient approximation (GGA) [17]. All calculations used a 2^3 Monkhorst-Pack k-point mesh [18]. The antisite formation energy was calculated by considering each antisite defect in separate simulation cells, mimicking infinite separation.

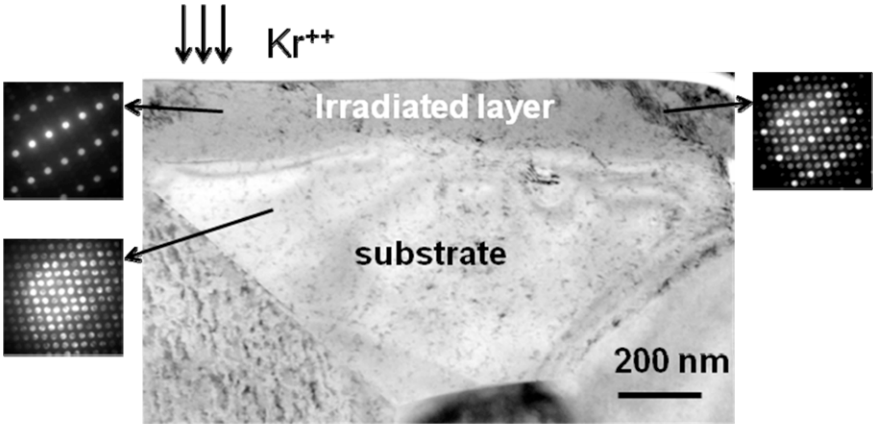

Fig. 2. Cross-sectional TEM bright-field image and microdiffraction (μD) patterns obtained from $Y_6U_1O_{12}$ irradiated to a fluence of 2×10^{20} Kr/m^2 (~50 dpa) at 100 K. The disappearance of specific diffraction spots (top μD patterns) suggests that there is a partial O–D phase transformation in the irradiated $Y_6U_1O_{12}$.

Based on DFT results, the cation antisite formation energies for $Y_6W_1O_{12}$, $Yb_6W_1O_{12}$, and $Y_6U_1O_{12}$ are 11.90, 10.25, and 8.21 eV, respectively. These are relatively large numbers, larger than equivalent energies found for other materials with empirical potentials [2,4]. This suggests that disordering might be relatively difficult in these materials. Nevertheless, the uranium δ-phase compound has a significantly lower cation antisite formation energy compared to the tungstate δ-phase compounds, which implies that cation disordering may occur more readily in δ-$Y_6U_1O_{12}$. In turn, this suggests that the uranate compound may be more difficult to amorphize than the tungstates. Work is in progress to improve these DFT simulations by including both anion and cation disorder in the calculations [19].

Though δ-$Y_6U_1O_{12}$ is found to exhibit impressive irradiation-induced amorphization resistance, it is important to note that we did not observe δ-$Y_6U_1O_{12}$ to readily undergo an ordered rhombohedral to disordered cubic fluorite transformation. In fact, this O–D transformation seems to be more pronounced in the δ-$Y_6W_1O_{12}$ and δ-$Yb_6W_1O_{12}$ compounds at similar ion doses. The antisite formation energy in the uranate compound is quite high, suggesting that this material strongly desires cation ordering. That a material with such a strong propensity for ordering does not amorphize under irradiation is interesting and challenges our previous understanding of amorphization resistance [2,4]. However, the ability of a material to accommodate disorder via mechanisms such as cation antisite formation is only part of the story for amorphization resistance. Also of key importance are the number and types of defects produced during irradiation and the kinetics associated with the migration and annihilation of these defects. Future work will investigate defect survivability and migration characteristics in these δ-phase materials.

In summary, we performed Kr^{++} ion irradiation experiments under cryogenic conditions (100 K) on polycrystalline δ-$Y_6U_1O_{12}$. GIXRD measurements and TEM observations revealed that δ-phase $Y_6U_1O_{12}$ possesses higher resistance to ion irradiation-induced amorphization than δ-$Y_6W_1O_{12}$ and δ-$Yb_6W_1O_{12}$. Theoretical simulations of cation antisite formation energies, performed using DFT, also support the hypothesis that δ-$Y_6U_1O_{12}$ should be more resistant to radiation damage than the surrogate tungstate compounds (δ-$Y_6W_1O_{12}$ and δ-$Yb_6W_1O_{12}$), due to its lower cation antisite formation energy. The significance of this study is that, to our knowledge, this is the first demonstration of significant radiation tolerance (specifically amorphization resistance) in a fluorite derivative compound containing a substantial actinide concentration and irradiated to a substantial dose (greater than 10 dpa). Fluorite derivatives such as pyrochlores ($A_2B_2O_7$) have long been touted as potential actinide waste or fuel forms; but here, we provide the first evidence, in an actinide-bearing compound, supporting these conjectures.

This work was sponsored by the Seaborg Institute for Transactinium Science, Los Alamos National Laboratory, and the US Department of Energy, Office of Basic Energy Sciences, Division of Materials Sciences and Engineering.

References

[1] W.J. Weber, R.C. Ewing, C.R.A. Catlow, T. Diaz de la Rubia, L.W. Hobbs, C. Kinoshita, H. Matzke, A.T. Motta, M. Nastasi, E.K.H. Salje, E.R. Vance, S.J. Zinkle, J. Mater. Res. 13 (6) (1998) 1434.
[2] K.E. Sickafus, L. Minervini, R.W. Grimes, J.A. Valdez, M. Ishimaru, F. Li, K.J. McClellan, T. Hartmann, Science 289 (2000) 748.
[3] R.C. Ewing, W.J. Weber, J. Lian, J. Appl. Phys. 95 (2004) 5949.
[4] K.E. Sickafus, R.W. Grimes, J.A. Valdez, A. Cleave, M. Tang, M. Ishimaru, S.M. Corish, C.R. Stanek, B.P. Uberuaga, Nat. Mater. 6 (2007) 217.
[5] E.A. Aitken, S.F. Bartram, E.F. Juenke, Inorg. Chem. 3 (1964) 949.
[6] S.F. Bartram, Inorg. Chem. 5 (1966) 749.
[7] H.J. Rossell, J. Solid State Chem. 19 (1976) 103.
[8] K.E. Sickafus, R.W. Grimes, S.M. Corish, A.R. Cleave, M. Tang, C.R. Stanek, B.P. Uberuaga, J.A. Valdez, Layered Atom Arrangements in Complex Materials, Los Alamos Series Report # LA-14205, 2006.
[9] J.F. Ziegler, J.P. Biersack, U. Littmark, The Stopping and Range of Ions in Solids, Pergamon, New York, 1985.
[10] A. Guinier, X-ray Diffraction in Crystals Imperfect Crystals and Amorphous Bodies, Dover Publications Inc., New York, 1994.
[11] D. Rafaja, V. Valvoda, A.J. Perry, J.R. Treglio, Surf. Coat. Technol. 92 (1997) 135.
[12] M. Tang, J.A. Valdez, K.E. Sickafus, J. Nucl. Mater. 376 (2008) 247.
[13] M. Tang, J.A. Valdez, K.E. Sickafus, CAARI 2008 proceeding.
[14] J.A. Valdez, M. Tang, K.E. Sickafus, Nucl. Instrum. and Meth. B 250 (2006) 148.
[15] G. Kresse, J. Hafner, Phys. Rev. B 48 (1993) 13115;
G. Kresse, J. Furthm, Comput. Mater. Sci. 6 (1996) 15;
G. Kresse, J. Furthm, Phys. Rev. B 54 (1996) 11169.
[16] G. Kresse, D. Joubert, Phys. Rev. B 59 (1999) 1758;
P.E. Blochl, Phys. Rev. B 50 (1994) 17953.
[17] J.P. Perdew, J.A. Chevary, S.H. Vosko, K.A. Jackson, M.R. Pederson, D.J. Singh, C. Fiolhais, Phys. Rev. B 46 (1992) 6671.
[18] H.J. Monkhorst, J.D. Pack, Phys. Rev B 13 (1976) 5188.
[19] C. Jiang, in preparation.